Journal of Engineering and Applied Sciences 8 (6): 183-191, 2013
ISSN: 1816-949X

Indirect Solar Drying Kinetics of Sheanut (*Vitellaria paradoxa* Gaertn) Kernels

[1, 3]Divine Nde Bup, [2]Charles Fon Abi, [3]Dzudie Tenin, [3]Cesar Kapseu,
[4]Clerge Tchiegang and [5]Zephirin Mouloungui
[1]Higher Institute of the Sahel, University of Maroua, P.O. Box 45, Maroua, Cameroon
[2]Department of Chemistry, Advanced Teachers' Training College,
University of Yaounde 1, P.O. Box 47, Yaounde, Cameroon
[3]Department of Process Engineering,
[4]Department of Food Science and Nutrition, ENSAI,
University of Ngaoundere, P.O. Box 455 Ngaoundere, Cameroon
[5]University de Toulouse, UMR 1010, Laboratoire de Chimie Agro-Industrielle,
ENSIACET, INP, INRA, 4 Allee Emile Monso, BP 74233 F-31432 Toulouse Cedex 4, France

Abstract: An indirect solar dryer was tested for drying sheanut kernels. The influence of tray distance from heat source, airspeed and particle size on drying kinetics was investigated. Optimum drying air parameters obtained in the dryer were airspeeds of 1 and 1.4 m sec^{-1} and a temperature of 40-45°C. Sheanut kernel slices dried entirely in the falling rate period. Drying rate decreased with increase in particle size. The effect of particle size on the drying rate suggested that the drying process was controlled by internal mass transfer. Drying kinetics was modeled with characteristic drying curve and diffusive models. Effective moisture diffusivities of sheanut kernel slices calculated without shrinkage were greater than those calculated with the incorporation of shrinkage by a value of about 50%. Acid and peroxide values indicated that butter from the dryer could be classified either as category 1 or 2 irrespective of the drying conditions to which the kernels were subjected.

Key words: Indirect solar drying, modelling, shrinkage, sheanut kernels, temperature

INTRODUCTION

Vitellaria paradoxa commonly called the shea tree is a multipurpose tree that grows in the wild in 17 countries of Sub-Saharran Africa. It produces fruits that each contains one large oval to slightly round, red brown to dark brown seed which is usually referred to as the sheanut (Maranz *et al*., 2003). The main importance of the shea tree is due to the fact that fat can be extracted from the dried kernels which is traditionally utilised in large quantities for cooking, as a moisturising cream and as a herbal medicine (Abbiw, 1990). The shea tree produces the second most important oil crop in Africa after oil palm but as it grows in areas unsuitable for palm, it takes on primary importance in West Africa and in regions where annual precipitation is <1000 mm of rainfall. Though, the tree is indigenuous to sub-Saharran Africa, it is used worldwide because 5% of the butter is used as cocoa butter replacers in chocolate equivalents. A very big market for sheanuts and butter exist in some European countries, Japan and the United States of America.

When shea fruits are mature, they are harvested or fall to the ground and are collected at a moisture content of 45-60%. This harvesting and/or collection falls within the maturation period (May to August) for other crops (a period when farmers are most busy with other farming activities). The shea fruit is therefore not given proper attention after harvest, since the other farming activities are considered primordial for the livelihood of the farmers and as such easily go bad. Sheanut kernel processing methods are typically traditional, tedious and un-mastered and often lead to low quality kernels and butter. Fresh sheanut kernels are big in size with average major, intermediate and minor diameters of 4.2, 2.8 and 2.4 cm, respectively (Bup *et al*., 2012). Kapseu *et al*. (2007) demonstrated that due to this large size, drying of whole kernels at 45°C took 12 days and equally led to the development of surface coat which hindered further drying suggesting that the kernels could be diced into smaller size before drying to shorten drying times. The popularly used sun drying method, though relatively cheap is long (5-20 days) and exposes the dried kernels to rain and attack by micro-organisms and insects.

Womeni reported that the treatment of shea kernels in a deep fat frying process significantly reduces the moisture content within a very short period of time.

Corresponding Author: Divine Nde Bup, Higher Institute of the Sahel, University of Maroua, P.O. Box 45, Maroua, Cameroon

However, this method will add to the huge quantity of wood consumed in the boiling of nuts and oil extraction stages.

Fruits and vegetables have high initial moisture contents and suffer alterations of their original form during the drying process due to significant shrinkage. Shea fruits contain 45-60% moisture content and are therefore likely to shrink during drying. These modifications occur continuously during the drying process and they affect the physical properties, as well as the transport phenomena. Thus, shrinkage has an influence on the drying rate and on the texture of dried foods (Hatamipour and Mowla, 2002; Talla *et al*., 2004). Work on the drying of sheanut slices and shrinkage of sheanut kernels is not reported in the literature.

From the foregoing, coupled with the high cost and absence of electricity in shea producing localities (which are mostly rural), this study is aimed at modeling the indirect solar drying behavior of the kernels with the incorporation of shrinkage for an eventual integration of the dryer into the shea kernel production process.

MATERIALS AND METHODS

Sheanut kernels: The sheanut kernels used in the drying process were obtained from Tchabal village in Ngaoundere, Cameroon and stored in a freezer at -18°C until analysis.

Description of the indirect solar dryer used: The indirect solar dryer used consisted of a solar collector, a drying chamber and an air evacuating system (Fig. 1). The solar collector is a flat box made of wood in the inner portions and covered with a 4 mm thick transparent glass material having a thermal conductivity of 0.9/Wm/k and density of 2.39 g cm^{-3}. The inner walls of the collector are lined with an undulating aluminium sheet and are painted black to promote energy absorption. The drying chamber contains 3 trays, each separated by a distance of 15 cm.

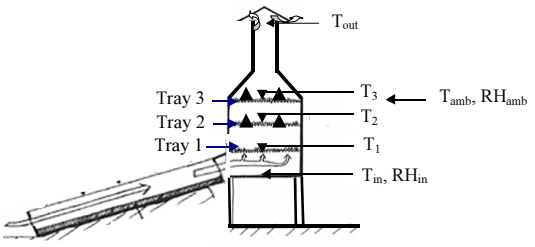

Fig. 1: A sketch of the dryer showing temperature measurements

The upper portion of the drying chamber is conical in shape and leads to the evacuating system (the chimney).

Drying kinetics: Sheanuts were cooked at 85±5°C for 120±5 min. Bup *et al*. (2012), manually cracked and the kernels cut into required slab thicknesses using a Tommy Slicer (model Siemens, Erlangen, Germany) (Fig. 2). The samples were then deposited on monolayer trays. These were then introduced into the dryer separately and the loss in weight with time recorded until a nearly constant mass of the sample was observed. In each drying, run the initial weight per monolayer tray was 10 g. The choice of this weight was based on the size of the monolayer tray which allowed uniform spread of the sample. The sample was weighed after every 30 min and quickly returned into the dryer using a digital balance of accuracy of 0.01 g. This took about 12-15 sec and was considered negligible on the overall experiment (Sankat *et al*., 1996; Kapseu *et al*., 2007). In all the drying runs, there were three small monolayer trays and from the tray replicates average values of the moisture content were determined as a function of time. These values were used to construct the drying curves.

Influence of airspeed on the drying kinetics of sheanut kernel: These studies were carried out on the 5 mm thick slices. To vary the airspeed, three blowers were installed at the entrance the collector. The 4 different airspeeds (natural convection, 0.6, 1 and 1.4 m sec^{-1}) were obtained

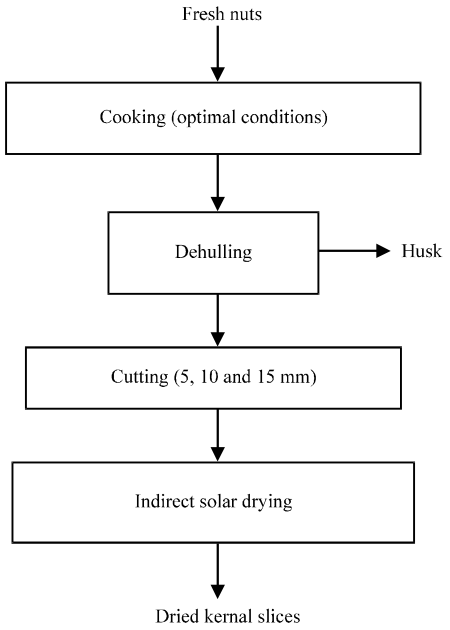

Fig. 2: Block diagram for the process of drying sheanut kernels to obtain butter

when 0-3 fans were on at a time and investigated in the dryer. At each airspeed, three smaller trays each loaded with the 10 g of the samples were deposited on each of the three larger trays for the drying kinetic study. These experiments were used to evaluate effect of tray distance from heat energy source on the drying rate of the kernels. The experimental plan here was 4×3. That is 4 airspeeds (natural convection, 0.6, 1 and 1.4 m sec^{-1}) and 3 tray distances (15, 30 and 45 cm) from energy source.

Influence of particle size on the drying kinetics: To evaluate the influence of particle size on the drying kinetics, the kernels were cut into 5, 10 and 15 mm thick slices and 10 g of each particle size placed in smaller trays and deposited on the first drying tray (15 cm from the solar collector in let) at each airspeed and the drying kinetics was followed. The 3 replicates were used for each particle size. The experimental plan was 3×3. That is 3 airspeeds (natural convection, 1 and 1.4 m sec^{-1}) and 3 particle sizes (5, 10 and 15 mm).

Modelling of the drying kinetics: The method of the Characteristic Drying Curve (CDC) and four semi empirical models based on the Fick's diffusion equation were selected and tested to model the drying kinetics of sheanut kernel slabs.

Method of the characteristic drying curve: This method represents the drying behavior of a material into a single curve called the characteristic drying curve which can be represented as:

$$V_r = \frac{V_t}{V_0} = f(X_r) \quad (1)$$

$$X_r = \frac{X - X_{eq}}{X_{cr} - X_{eq}} \quad (2)$$

This curve is independent of parameters, such as temperature, air velocity, particle thickness, heat and mass transfer coefficients:

Where:

X_{eq} = The equilibrium moisture content determined experimentally or by desorption
X_{cr} = The critical moisture content considered as the initial moisture content
X_0 = In the case of biological products where the absence of the constant rate drying period is common
V_0 = The rate of drying in the first phase of drying
V_r = The normalised drying rate
V_t = The drying rate at time t

A modified version of the characteristic drying curve for biological products has been described by Ahouannou as follows:

$$X = X_{eq} + \left[\left(X_0 - X_{eq}\right)^{(1-q)} + \frac{V_0(1-q)}{\left(X_0 - X_{eq}\right)^{q}} t \right]^{\frac{1}{1-q}} \quad (3)$$

Where:

q = The characteristic drying coefficient of the product
X = The moisture content at time t
q = The calculated from the equation

$$q = \frac{1}{N_d} \sum_{i=1}^{N_d} \left[\frac{1}{p} \sum_{i=1}^{p} \left(\frac{\ln V_r}{\ln \varphi} \right)_t \right] \quad (4)$$

Where:

N_d = The number of drying runs
p = The number of points at which moisture content is measured

The CDC model necessitates the determination of the following constants:

Rate of drying in the constant rate drying phase (V_0): In the absence of the constant rate drying period, it is defined by the initial drying rate which was determined from experiments after the first 30 min of drying.

Initial moisture content (X_0): This was obtained by the oven method before each drying run.

The equilibrium moisture content (X_r): The equilibrium moisture contents were obtained from sorption isotherms of sheanut kernels (Bup *et al*., 2012).

The characteristic drying coefficient (q): This was determined from Eq. 4.

Models based on the Fick`s diffusion equation: The 4 semi empirical models (Table 1); Page, Modified Page, Henderson and Pabis and Lewis which are based on the solution of the Fick's diffusion equation for a slab (Eq. 5):

$$\frac{\partial X}{dt} = D\nabla^2 X \quad (5)$$

Table 1: Diffusive models tested for modelling the drying kinetics of sheanut kernel slices

Name of model	Model	References
Lewis	$X_r = \exp(-K_l t)$	Lewis (1921)
Henderson and Pabis	$X_r = a \exp(-K_{hp} t)$	Henderson and Pabis (1961)
Page	$X_r = \exp(-K_p t^m)$	Page (1949)
Modified Page	$X_r = \exp(-(K_{mp} t)^m)$	White *et al*. (1981)

X_r = The removal moisture content

were also used to describe the drying behaviour of the kernels. The drying constants K from the Lewis and Henderson and Pabis equation were obtained from the slopes of the plots of ln (X_r) against t while those from the Page and Modified Page equations were obtained from the slopes of ln (-lnX_r) against ln (t).

Modeling with shrinkage: To consider the effect of shrinkage in modeling, the Fick's diffusion equation:

$$\frac{\partial X}{dt} = D\nabla^2 X \tag{6}$$

was considered. Adding the density of dry solid, ρ_s, to both sides of Eq. 7 gave:

$$\frac{\partial(\rho_s X)}{dt} = D_{eff}\nabla^2(\rho_s X) \tag{7}$$

Or for a constant weight dry solid, X_s (Park, 1998) where $\rho_s = X_s/V$:

$$\frac{\partial X_s\left(\frac{X}{V}\right)}{dt} = \frac{X_s\partial\left(\frac{X}{V}\right)}{dt} = X_s D_{eff}\nabla^2\left(\frac{X}{V}\right) \tag{8}$$

Substituting W = X/V in Eq. 8, researchers have:

$$\frac{\partial W}{dt} = D_{efsh}\nabla^2 W \tag{9}$$

With:

$$t-0; X = \frac{X_0}{V_0}$$

$$t>0; z=0; \frac{\partial X}{\partial z} = 0$$

$$t>0; z=l; W_{eq} = \frac{X_{eq}}{V_{eq}}$$

Considering that the solution to the Fick's diffusion equation for a slab without shrinkage is normally given by:

$$X_r = \frac{X-X_{eq}}{X_0-X_{eq}} = \frac{8}{\pi^2}\sum_{n=0}^{n=\infty}\frac{1}{(2n+1)} + \exp\left[-(2n+1)^2\pi^2 D_{eff}\frac{t}{4l^2}\right] \tag{10}$$

Then, the solution to the Fick's diffusion equation for a slab including shrinkage is given by:

$$Y_r = \frac{W-W_{eq}}{W_0-W_{eq}} = \frac{8}{\pi^2}\sum_{n=0}^{n=\infty}\frac{1}{(2n+1)^2} + \exp\left[-(2n+1)^2\pi^2 D_{efsh}\frac{t}{4l^2}\right] \tag{11}$$

Where:

$D_{eff\ and\ efsh}$ = The effective moisture diffusivities ($m^2\ sec^{-1}$) with and without shrinkage, respectively
V = The sample volume (m^3)
V_{eq} = The equilibrium volume obtained from the shrinkage equation at X = X_{eq} (Bup *et al*., 2011)
l = The thickness of the particle under consideration in metres n = {0, 1, 2, ...} and defines the number of terms in Eq. 10 and 11

Determination of the effective moisture diffusivities: The effective moisture diffusivities with and without shrinkage were determined from Eq. 11 and 12 by plotting values of ln (X_r) and ln (W_r), respectively against time (for n = 0) as a function of airspeed and particle size.

Validation of models: The criteria for evaluating the reliability of the simulations were the regression coefficients and/or the standard relative error of deviation observed on the moisture content between the experimental and theoretical results. The Standard Relative Error (SRE) of deviation of theoretical from experimental results was determined from Eq. 12:

$$SRE(\%)\frac{100}{n}\sum_{i=1}^{n}\left|\frac{X_{exp}-X_{mod}}{X_{exp}}\right| \tag{12}$$

Where:

X_{exp} = The values obtained from experiments
X_{mod} = The values obtained from the model
P = The number of points at which measurements were carried out

RESULTS AND DISCUSSION

Drying kinetics: During the test period average ambient Temperature (T_{amb}) and Relative humidity (R_{amb}) varied from 19-27°C and 50-90%, respectively. The corresponding average air drying conditions obtained in the drying chamber were 29-51°C and 31-65%, respectively. The differences obtained between ambient and drying chamber air temperatures and relative humidities ranged from 5-24°C and from 19-31%, respectively indicating clearly that the air in the dryer had a higher drying efficiency.

As expected, water content of the sample decreased with time until, it reached a critical value for all the drying

runs. Irrespective of the environmental conditions under which drying was carried out, the constant drying phase was absent for all the drying runs (Fig. 3). That is, drying was observed to occur generally in the falling rate period. This is in conformity with the drying of agricultural or biological products where the absence of the constant rate period is generally observed. The absence of the constant drying phase has been observed for the electric drying of sheanut kernel slices (Kapseu *et al*., 2007) and for bananas (Sankat *et al*., 1996).

Influence of airspeed: The 4 different airspeeds (natural convection, 0.6, 1 and 1.4 m sec^{-1}) were investigated. Figure 4-7 show the influence of airspeed on the drying kinetics of 5 mm thick kernel slices, dried on tray 1-3 under the same environmental conditions for each airspeed. These trays were located at 15, 30 and 45 cm, respectively from the solar collector end. In Fig. 4 when the solar dryer ran under natural convection, the samples on tray 1 which were closest to the collector dried faster than those on trays 2 and 3. This was probably due to the accumulation of heat around the tray which lacked the necessary force to push it up through trays 2 and 3.

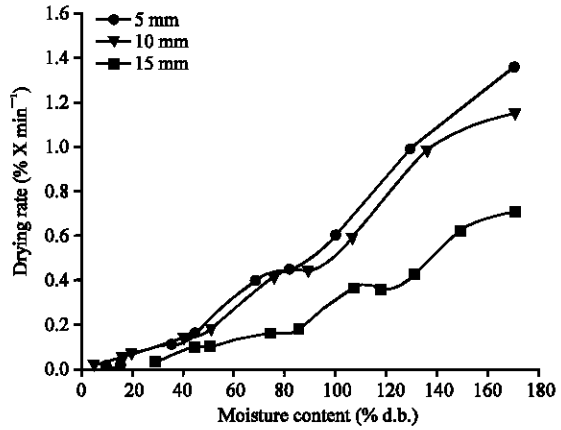

Fig. 3: Drying rate curves for sheanut kernel slices; 1 m sec^{-1}; T_{amb} = 19-27°C; T_{in} = 30-40°C

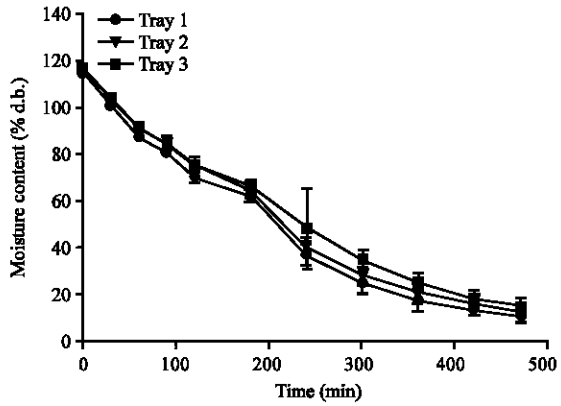

Fig. 4: Influence of tray distance from the drying air inlet on the drying kinetics under natural convection

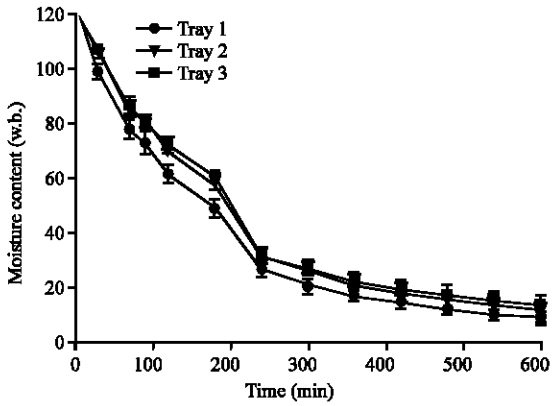

Fig. 5: Influence of tray distance from the drying air intel on the kinetics at 1 m sec^{-1}

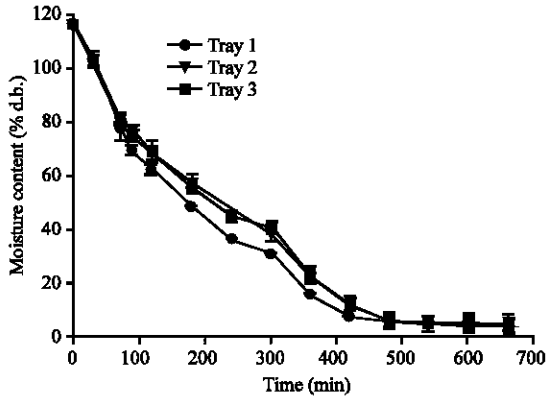

Fig. 6: Influence of tray distance from the drying air inlet on the drying kinetics at 1.4 m sec^{-1}

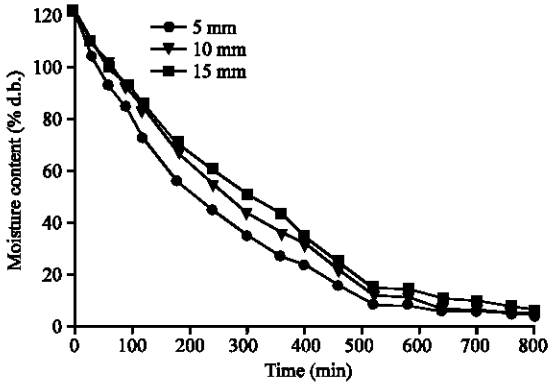

Fig. 7: Influence of particle size on the indirect solar drying kinetics of sheanut kernel slices under natural convection

When air was forced into the solar dryer, samples on trays 2 and 3 dried virtually at the same time (Fig. 5-7). The differences in the moisture content at a given time of the samples on trays 1 and 2 or 3 became smaller compared to difference obtained when the samples were dried under natural convection. This difference in the moisture content at a given time between trays decreased as the airspeed increased. Drying on trays 2 and 3 was slower compared to that on tray 1 at all airspeeds. For example, the drying constant obtained from the Modified Page (Table 2) equation at 1 m sec^{-1} for the 5 mm thick slice on tray 1 (0.0063% water min^{-1}) was significantly higher than those obtained on tray 2 (0.0052% water min^{-1}) and on tray 3 (0.0050% water min^{-1}). There was, however no significant difference on the moisture content of the kernels dried on different trays towards the end of the drying process at all airspeeds. Hence, drying could be carried out on any of the trays to give the same moisture content at the end of drying.

Influence of particle size on the drying kinetics of sheanut kernels: The influence of particle size on the drying kinetics of sheanut kernels under different ambient conditions and airspeeds are presented in Fig. 8-10. As expected, the drying rate (Fig. 3) decreased with an increase in particle size. Hence, the 5 mm thick slices gave higher drying rates compared to the 10 and 15 mm thick slices. The effect of particle size on the drying rate as observed suggested that the drying process was controlled by internal mass transfer (Waananen, 1989). The effect of particle size was more pronounced and distinct when the particles were dried at 1.4 m sec^{-1} (Fig. 10) where temperatures were lowest. The ambient air Temperatures (T_{amb}) during the evaluation on the respective days ranged from 21-25, 21-27 and 19-27°C for natural convection, 1 and 1.4 m sec^{-1} runs. The corresponding values for air temperatures in the drying chamber were 29-51, 30-46 and 31-40°C, respectively. The drying constants obtained from the Modified Page model (Table 2) for the 5, 10 and 15 mm thick slices under natural convection were 0.0047, 0.0036 and 0.003, respectively. The corresponding values at 1 m sec^{-1} were 0.0078, 0.0069 and 0.0039 (Table 3). At 1.4 m sec^{-1}, these values decreased to 0.0055, 0.0037 and 0.0022 (Table 4). These drying constants were, therefore more dependent

Table 2: Model constants and R^2 and SRE values for tested diffusive models under natural convection

	Page					Henderson and Pabis		
Particle size (mm)	K_p or K_{mp}	m_p or m_{mp}	R^2	SRE	A	K_{hp} or K_l	R^2	SRE
5	0.0052	0.98	0.997	37.10	1.04	0.0049	0.997	5.76
10	0.0024	1.08	0.998	27.20	1.06	0.0040	0.994	5.77
15	0.0033	1.00	0.994	2.61	1.04	0.0035	0.992	5.53
	----------Modified page----------					----------Lewis---------		
5	0.0047	0.98	0.997	3.93		0.0049	0.9970	6.70
10	0.0036	1.08	0.998	3.79		0.0040	0.9938	8.39
15	0.0033	1.00	0.994	5.34		0.0035	0.9924	6.40

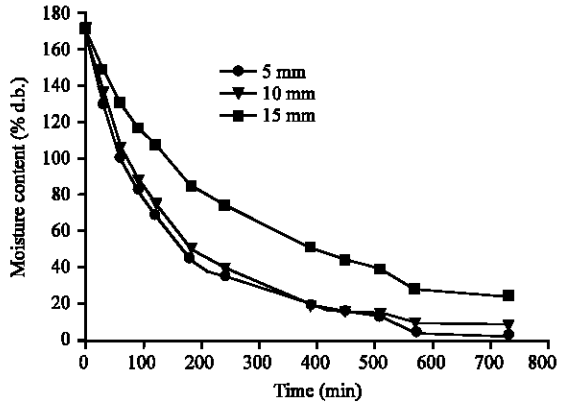

Fig. 8: Influence of particle size on the indirect solar drying kinetics of sheanut kernel slices 1 m sec^{-1}

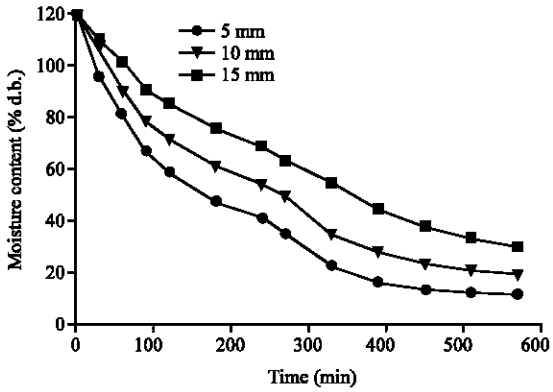

Fig. 9: Influence of particle size on the indirect solar drying kinetics of sheanut kernel slices at 1.4 m sec^{-1}

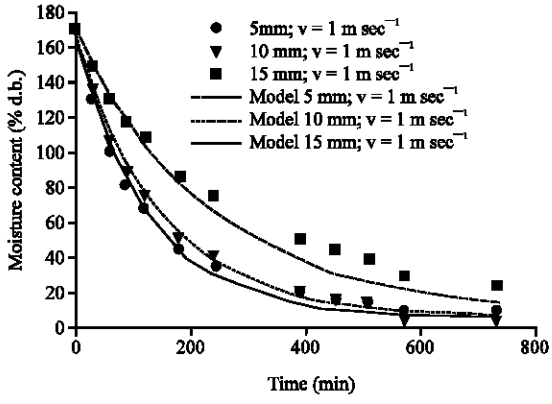

Fig. 10: Comparison of experimental and theoretical drying curves using parameters of the CDC

Table 3: Model constants and R^2 and SRE values for tested diffusive models 1 m sec^{-1}

	Page					Henderson and Pabis		
Particle size (mm)	K_p or K_{mp}	m_p or m_{mp}	R^2	SRE	A	K_{hp} or K_l	R^2	SRE
5	0.0181	0.83	0.998	3.64	0.83	0.0058	0.980	8.25
10	0.013	0.87	0.999	7.93	0.84	0.0054	0.985	9.26
15	0.0081	0.85	0.999	3.36	0.91	0.003	0.989	5.39
	----------Modified page---------					---------Lewis----------		
5	0.0078	0.83	0.998	3.64		0.0058	0.975	22.70
10	0.0069	0.87	0.999	7.93		0.0054	0.985	21.80
15	0.0035	0.85	0.999	3.36		0.0030	0.989	11.10

Table 4: Model constants and R^2 and SRE values for the tested diffusive models at 1.4 m sec^{-1}

	Page					Henderson and Pabis		
Particle size (mm)	K_p or K_{mp}	m_p or m_{mp}	R^2	SRE	A	K_{hp} or K_l	R^2	SRE
5	0.0152	0.80	0.995	6.95	0.94	0.0055	0.989	8.93
10	0.0075	0.87	0.992	4.95	0.95	0.0038	0.989	6.16
15	0.0049	0.89	0.995	3.09	0.98	0.0027	0.995	2.87
	----------Modified page----------					----------Lewis----------		
5	0.0055	0.80	0.995	6.96		0.0055	0.989	11.50
10	0.0037	0.87	0.992	4.95		0.0038	0.989	7.94
15	0.0022	0.87	0.996	7.90		0.0027	0.994	3.50

on temperature rather than on airspeed, since they decreased with an increase in temperature. From the drying constants, it could be concluded that the higher drying chamber air temperatures obtained for natural convection and at 1 m sec^{-1} airspeed had a more pronounced effect on the drying rates which were reflected in their drying constants, compared to the airspeed. This perhaps explained why the influence of particle size was more discernible at 1.4 m sec^{-1} where drying chamber air temperatures were lowest.

Modelling of the drying kinetics

The characteristic drying curve model: The drying rate in the constant period was taken as the initial rate of drying due to the absence of the constant rate period. Equally the initial moisture content was taken as the critical moisture content for the same reason. Table 2 gives the various constants obtained for the drying of sheanut kernel slices under different experimental conditions for the characteristic drying curve model. An example of the superimposition of the experimental and the theoretical drying curves resulting from the characteristic drying curves for different particle sizes is shown in Fig. 11. The average value of the characteristic drying constant q, obtained for different particle sizes dried at 1 and 1.4 m sec^{-1} in the temperature ranges 30-46 and 31-40°C, respectively was 1.01. This value which was slightly >1 suggested that the drying process, especially towards the end of the process was slow and was diffusion controlled.

The high average R^2 (0.993) and SRE (10.4%) values, the close fit between experimental and theoretical curves

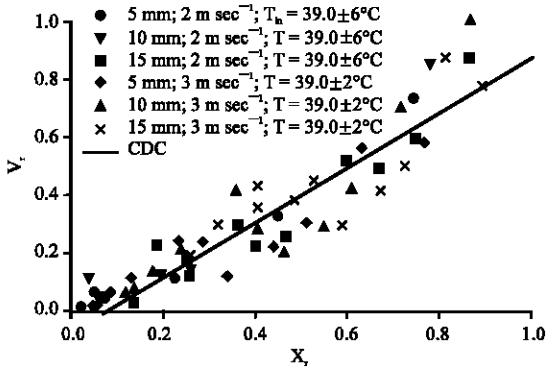

Fig. 11: CDC obtained for differrent drying runns

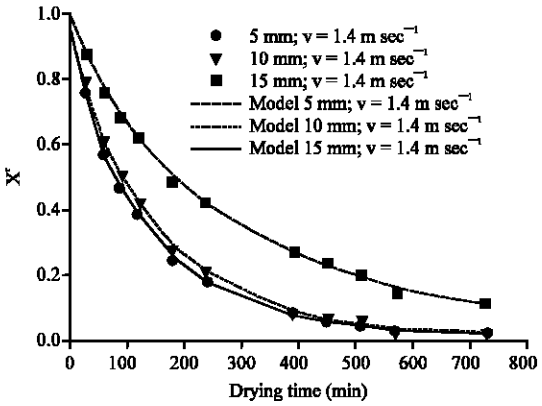

Fig. 12: Comparison of experimental with theoratical drying curves using parameters of the Modified Page model

(Fig. 11) as well the regrouping of the experimental drying curves around the CDC (Fig. 12) suggested that this model was adequate for describing the indirect solar drying behaviour of sheanut kernels.

Models based on the Fick's diffusion equation: Model constants and R^2 and SRE values for the Page, Modified Page, Henderson and Pabis and Lewis are presented on Table 2 and 4. These values show the Modified Page model described best the drying behaviour of the sheanut kernel slices as confirmed by Fig. 12. From Table 2 and 4, the values of the drying constants, K were dependent on the particle size increasing with a reduction in particle size. All the semi empirical models tested indicated drying to occur only in one phase in the falling rate period which gave rise to one drying constant for each treatment.

Effective moisture diffusivities of the sheanut kernel slices

Influence of airspeed on the effective moisture diffusivities of the kernels: The variation of effective

moisture diffusivities without shrinkage (D_{eff}) of sheanut kernels dried on trays located at different distances from the collector (heated air inlet) with airspeed are presented in Fig. 12. These studies were carried out on a separate day at each airspeed where the ambient and drying, air temperatures and relative humidities were characteristic of the day. This may explain why the pattern of variation of D_{eff} with airspeed is not regular. At each airspeed, 3 smaller trays, each containing 10 g of 5 mm thick samples were deposited on the different larger drying trays. These were then dried under the same conditions, so their D_{eff} values at the 3 different distances for a particular airspeed could be compared. Under natural convection, the difference between the D_{eff} on the three trays was very significant. This difference decreased significantly with an increase in airspeed, especially between trays 1 and 2 which were at distances of 30 and 45 cm from the solar collector, respectively (Fig. 13). The relatively higher values of D_{eff} obtained at 0.6 m sec^{-1} could be due to the higher drying chamber air temperatures recorded on this day (29-51°C). At lower airspeeds (natural convection and 0.6 m sec^{-1}), sufficient air was not available to take up the heated air accumulated at the collector into the drying chamber and consequently much heat was concentrated on tray 1 which was closest to the collector explaining the abnormal high value of D_{eff} on tray 1 under natural convection and at 0.6 m sec^{-1} as presented in Fig. 13. At 1.4 m sec^{-1}, the difference in D_{eff} between the 3 trays was greatly reduced indicating that at this airspeed, the product could be dried uniformly on the different trays.

Influence of particle size on the effective moisture diffusivities of the kernels with and without volumetric shrinkage: The effective moisture diffusivities of sheanut kernels slices evaluated with and without volumetric shrinkage are presented in Fig. 14. The effective moisture diffusivities of the samples decreased with an increase in particle size irrespective of the ambient drying chamber air conditions. The irregular pattern of variation observed with respect to different airspeeds could be explained by the differences in the ambient and drying chamber air temperatures and relative humidities under which the different drying tests were carried out.

The effective moisture diffusivities of the samples ranged from 2.74×10^{-8} to 5.88×10^{-8} m^2 sec^{-1} and from 1.62×10^{-8} to 4.4×10^{-8} m^2 sec^{-1} with and without shrinkage, respectively. With the incorporation of shrinkage, the effective moisture diffusivities were reduced by 42.86, 52.50 and 45.75% for the 5, 10 and 15 mm samples dried under natural convection.

This reduction in effective moisture diffusivities brought about by the incorporation of volumetric shrinkage indicated that the assumption of no shrinkage during the drying of agricultural products as often done in the literature (Arevalo-Pinedo and Murr, 2006) over estimated effective moisture diffusivity values. The percentage difference in effective moisture diffusivities calculated without volumetric shrinkage between the 5 and 15 mm thick slices for samples dried under natural convection was 28.5. The corresponding values obtained at 1 and at 1.4 m sec^{-1} were 48.2 and 50.9%, respectively. At 1.4 m sec^{-1}, the difference was almost double that obtained under natural convection indicating that the introduction of blowers actually had a pronounced influence on the drying kinetics of the sheanut kernels slices as exemplified in the D_{eff} values. These results highlight the importance of incorporating shrinkage in the drying equations of sheanut kernels to predict drying times.

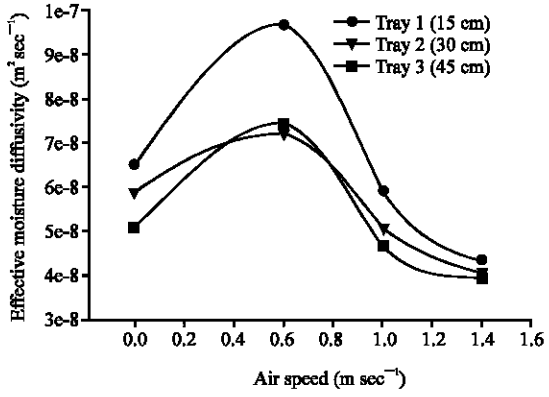

Fig. 13: Variation of effective moisture diffusivities with airspeed of 5 mm thick sheanut kernel slices deposited on different drying trays

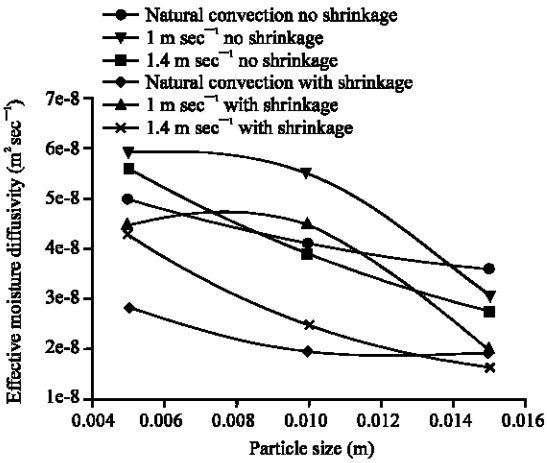

Fig. 14: Variation of effective moisture diffusivities with particle size at different airspeeds with and without shrinkage

CONCLUSION

The solar dryer studied has potential to dry sheanut kernels. At airspeeds of 1 and 1.4 m sec^{-1}, there was no significant difference in the moisture contents of the samples on the different trays due to the homogenization of the air drying temperature in the drying chamber. The model of the characteristic drying curve and four semi-empirical models were successfully used to model the indirect solar drying kinetics of sheanut kernels. Effective moisture diffusivities calculated with the incorporation of the shrinkage model gave values that were up to 50% less than those calculated without shrinkage. Shrinkage is an important parameter that should not be neglected in modeling drying of sheanut kernels.

REFERENCES

Abbiw, D.K., 1990. The Useful Plants of Ghana. Intermediate Technology Publications, Royal Botanic Gardens, London, UK.

Arevalo-Pinedo, A. and F.E.X. Murr, 2006. Kinetics of vacuum drying of pumpkin (*Cucurbita maxima*): Modeling with shrinkage. J. Food Eng., 76: 562-567.

Bup, D.N., N. Diarrasouba, C. Kapseu, D. Tenin, Kuitche, C.F. Abi and C. Tchiegang, 2011. Physical Properties of Shea (*Vitellaria Paradoxa* Gaertn.) Fruits, Nuts and Kernels from different Localities of Cameroon. In: Nuts, Properties and Consumption, Davis, I. (Ed.). Nova Book Publishers, Inc., New York, USA., pp: 129-150.

Bup, N.D., F.C. Abi, D. Tenin, C. Kapseu and C. Tchiegang, 2012. Optimisation of the cooking process of sheanut kernels (*Vitellaria paradoxa* Gaertn.) using the doehlert experimental design. Food Bioprocess Tech., 5: 108-117.

Hatamipour, M.S. and D. Mowla, 2002. Shrinkage of carrots during drying in an inert medium fluidized bed. J. Food Eng., 55: 247-252.

Henderson, S.M. and S. Pabis, 1961. Grain drying theory I. Temperature effect on drying coefficient. J. Agric. Eng. Res., 6: 169-174.

Kapseu, C., D.N. Bup, C. Tchiegang, F.C. Abi, F. Broto and M. Parmentier, 2007. Effect of particle size and drying temperature on drying rate and oil extracted yields of *Buccholzia coriacea* (Mvan) and *Butyrospermum parkii* ENGL. Int. J. Food Sci. Tech., 42: 573-578.

Lewis, W.K., 1921. The rate of drying of solid materials. Ind. Eng. Chem., 13: 427-432.

Maranz, S., Z. Wiesman and N. Garti, 2003. Phenolic constituents of shea (*Vitellaria paradoxa*) kernel. J. Agric. Food Chem., 51: 6268-6273.

Page, G., 1949. Factors influencing the maximum rates of air-drying shelled corn in thin layers. M.Sc. Thesis, Purdue University, Lafayette, IN., Illinois, USA.

Park, K.J., 1998. Diffusional model with and without shrinkage during salted fish muscle drying. Drying Technol. Int. J., 16: 889-905.

Sankat, C.K., F. Castaigne and R. Maharaj, 1996. The air drying behaviour of fresh and osmotically dehydrated banana slices. Int. J. Food Sci. Technol., 31: 123-135.

Talla, A., J.R. Puiggali, W. Jomaa and Y. Jannot, 2004. Shrinkage and density evolution during drying of tropical fruits: Application to banana. J. Food Eng., 64: 103-109.

Waananen, K.M., 1989. Analysis of mass transfer mechanisms during drying of extruded Pasta. Ph.D. Thesis, Purdue University, USA.

White, G.M., I. Ross, J. Ponelert and R. Fully, 1981. Fully exposed drying of popcorn. Transact. ASAE, 24: 466-468.